Monitoring the Spatiotemporal Distribution of Invasive Aquatic Plants in the Guadiana River, Spain

Elena C. Rodríguez-Garlito, *Student Member, IEEE*, Abel Paz-Gallardo, and Antonio Plaza, *Fellow, IEEE*

***Abstract*—Monitoring the spatiotemporal distribution of invasive aquatic plants is a challenge in many regions worldwide. One of the most invasive species on Earth is the water hyacinth. These plants are harmful to biodiversity and create negative impacts on society and economy. The Guadiana river (one of the most important ones in Spain) has suffered from this problem since the early 2000s. Several efforts have been made to mitigate it. However, invasive plants, such as the water hyacinth, are still present in seed banks at the bottom of the river and can germinate even more than a decade after. In this article, we propose an automatic methodology, based on remote sensing and deep learning techniques, to monitor the water hyacinth in the Guadiana river. Specifically, a multitemporal analysis was carried out during two years using images collected by ESA's Sentinel-2 satellite, analyzed with a convolutional neural network. We demonstrate that, with our strategy, the river can be monitored every few days, and we are able to automatically detect the water hyacinth. Three experiments have been carried out to predict the presence of water hyacinth from a few scattered training samples, which represent invasive plants in different phenological stages and with different spectral responses.**

***Index Terms*—Deep learning (DL), invasive aquatic species, multitemporal remote sensing, water hyacinth.**

I. Introduction

THE water hyacinth (*eichhornia crassipes*) is an aquatic perennial macrophyte native to Brazilian habitats [1]. This aquatic plant (that floats freely on the surface of freshwater) has spread to different parts of the world [2], being distributed in more than 50 countries across five continents. These species, considered as a valuable resource with several qualities [3], exhibit unique properties. Some authors have emphasized the ecological and socioeconomic application of the water hyacinth [4]. It absorbs heavy metals and organic contaminants, allowing its utilization in wastewater treatments [5], [6], [7] and for heavy metal removal [8], [9]. It also has potential use as water hyacinth biomass in biochar [10], bio-oil, and syngas [11]. Its use is also common in energy production, water treatment, agriculture (as a chemical and biological resource), and as an alternative to conventional construction materials [12]. However, its presence threatens the environment and produces a negative socioeconomic impact [13].

With high toleration in extreme environmental conditions [14], it outcompetes native vegetation, therefore affecting biodiversity. Moreover, climate change makes native plant species more vulnerable, also favoring invasive plant species that adapt better to changes. As a result, the water hyacinth is considered as one of the worst invasive alien species, and it is included in the Global Invasive Species Database [15]. The highly invasive nature of this plant is due, in part, to its rapid reproductive capacity (it can double its biomass in 6–12 days [16]). The plant is generally distributed in floating mats in the surface of rivers. These dense mats negatively affect important physiochemical water quality parameters. Dissolved oxygen concentration (the most important variable for aquatic fauna) is reduced with the growth of invasive plants [17], [18]. The patches that cover the water block the light needed for photosynthesis by other submersed vegetation. These patches also absorb nutrients from the water (impacting on ecological communities as well), decreasing phytoplakton distribution, and changing zooplankton abundance and diversity [19].

Water hyacinth invasion also creates a negative impact on different human activities, such as navigability, boating access, and recreation [20]. From an economic perspective, the invasion of hyacinth entails high costs in management [21], equipment, treatment, and qualified personnel for the tasks of control, removal, and elimination in the affected water bodies [22], [23], [24]. Given the difficulty of eradicating the invasive plants in affected watercourses, management efforts are aimed at reducing their biomass through various strategies. For this purpose, mechanical control or manual removal have been used [25], along with chemical [26], [27] or biological control [28], [29].

There is a legal framework in Europe that discourages a profitable economy around this kind of invasive species, prohibiting possession, and trade and trafficking of live specimens. Confederación Hidrográfica del Guadiana (CHG) is a public Spanish organization in charge of managing the Guadiana river basin. As shown in Fig. 1, the water hyacinth first appeared (following a tapestry-like distribution) in the Guadiana river

Manuscript received 30 September 2022; revised 5 November 2022; accepted 24 November 2022. Date of publication 28 November 2022; date of current version 7 December 2022. This work was supported in part by European Social Fund (Resolución de 10 de mayo de 2017, de la Secretaría General de Ciencia, Tecnología e Innovación, por la que se resuelve la convocatoria de ayudas para la financiación de contratos predoctorales para formación de Doctores en los centros públicos de I+D pertenecientes al Sistema Extremeño de Ciencia, Tecnología e Innovación en el ejercicio 2017, expediente PD16001), in part by Consejería de Economía, Ciencia y Agenda Digital of the Junta de Extremadura, in part by European Regional Development Fund (ERDF) of the European Union under Grant GR21040, in part by Spanish Ministerio de Ciencia e Innovacion under Project PID2019-110315RB-I00 (APRISA), and in part by European Union's Horizon 2020 Research and Innovation Program under Grant 734541 (EOXPOSURE). *(Corresponding author: Elena Cristina Rodríguez-Garlito.)*

The authors are with the Hyperspectral Computing Laboratory, Department of Technology of Computers and Communications, Escuela Politécnica, University of Extremadura, 10003 Cáceres, Spain (e-mail: elenacristinarg@unex.es; apazgal@unex.es; aplaza@unex.es).

Digital Object Identifier 10.1109/JSTARS.2022.3225201

Fig. 1. Water hyacinth (*Eichornia crassipes*) being removed by machinery in the Guadiana river, Spain.

basin in 2004, causing negative impacts as discussed above. This plant has also affected recreational activities in the Guadiana river, such as canoeing, as it completely invades sections of the river. Its accumulation on the piers affects navigation.

Several strategies have been adopted to mitigate the negative impact of invasive plants, with large economic investments. Some of these actions have been focused on manual and mechanized removals. Control infrastructures (such as containment and removal barriers) have been created. However, the Spanish legislation does not allow the use of herbicides in natural watercourses. In 2021, it was reported that a total of 150 783 092 tons of hyacinth were extracted since 2005 [30]. Surveillance activities have also been carried out to prevent its proliferation and expansion. The current focus is on control and early detection. Economic analyses have been conducted to demonstrate the benefits to the ecosystem of invasive species management [31]. In this way, an investment of 27 800 000 € has been foreseen for water hyacinth control and eradication measures for the 2021–2027 period.

The reproductive biology of water hyacinth allows for sexual and asexual reproductions [32], [33]. Asexual reproduction, through the formation of stolons, is the main cause of the rapid spread of water hyacinth [34]. On the other hand, sexual reproduction from a seed bank is also possible [35], [36]. According to reports from CHG, total elimination of the water hyacinth from the surface of the Guadiana river was accomplished on December 2020 [30]. However, the seeds still remain at the bottom of the river and they can germinate after a few years [35]. An important aspect to control their reproduction is early detection, allowing to taking removal measures. Invasive water species have a great capacity to reproduce and adapt to the environment in which they develop. Consequently, continuous monitoring and control of affected areas is necessary.

The seasonal growth of water hyacinth in Brazil was studied in [37], suggesting tactics for managing hyacinth with herbicide applications. The phenology and growth stages of the plant were described in a study conducted in a lake in Florida [38]. There, it was concluded that its growth phases exhibit adaptivity to the environment, ease of dispersal, reproduction, and repopulation after severe losses (particularly, in winter). Therefore, it is important to understand the phenological behavior of the plant and the

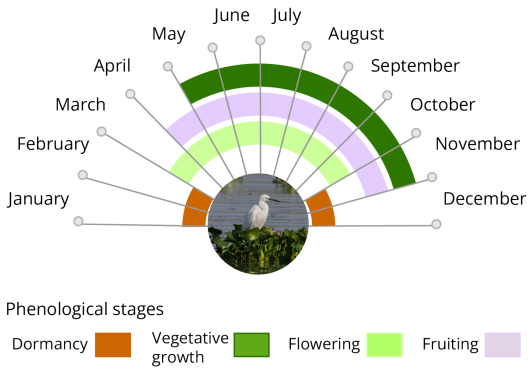

Fig. 2. Illustration of the phenological stages of water hyacinth in the Guadiana river, Spain.

dynamics of the changes it undergoes over time. Fig. 2 shows the phenology of water hyacinth in the Guadiana river basin (Spain). This figure has been elaborated from published reports by the CHG [30], [39], using field observations. It is important to note that the behavior shown in Fig. 2 can vary according to climatic aspects. In May, the vegetative growth period usually begins; the rapid development of the plant facilitates its asexual reproduction, which is capable of multiplying individuals in a very short time. Flowering usually begins in April and continues throughout the summer months. The flowers are blue and remain open from two to five days [40]. Flowering continues throughout the warm months and increases in June and August. After flowering, the fruit is produced. In November or December, the plants begin their dormancy period.

The main goal of this study is to develop a new technique to automatically detect and monitor the water hyacinth every five days [Sentinel-2 (S2) satellite revisit time] in a time series of remote sensing images spanning two years. Our aim is to determine seasonal changes in the spatial and temporal distributions of its biomass. We also analyze how many remote sensing images are required to collect suitable training samples for automatically detecting water hyacinth in the considered time series. Our goal is to minimize the number of images needed to obtain an accurate geolocation of the plant; thus, being able to model its phenological cycle. Specially, in this study we give particular

importance to accurately mapping the water hyacinth during the vegetative growth and propagation phases of the invasive plant. The main contributions of our work can be summarized as follows.

1) Following our previous work in [41], a deep learning (DL) model capable of identifying automatically water hyacinth has been selected as a baseline for evaluating the multitemporal evolution of the plant in a two-year time series. The selected model is able to discriminate invasive plants from the rest of the land cover, separating them from other types of vegetation.
2) A careful training of the DL model has been carried out by minimizing the number of samples collected. In this way, training samples have been extracted from only four multispectral S2 satellite images. Such training allows us to predict the presence of water hyacinth (in a two-year period) independently of the different phenological stages of the plant.
3) Using the trained model, we can monitor the spatiotemporal distribution of aquatic invasive plants every few days. This is accomplished by using S2 data (which allows obtaining an image over any location in the world every five days) without the need to retrain the model (i.e., by reusing the same training) with no additional cost in terms of image acquisition.

The rest of this article is organized as follows. Section II describes some related works. Section III explains the materials and methods used in our work. Section IV justifies the experimental design, shows the experimental results, interprets the water hyacinth dynamics, and assesses the adopted convolutional neural network (CNN) model. Section V discusses the obtained experimental results. Finally, Section VI concludes this article with some remarks and hints at plausible future research lines.

II. Related Works

In recent years, there has been an increase in the use of remote sensing techniques for mapping and monitoring water hyacinth. Different remote sensing instruments (such as Landsat Thematic Mapper, MODIS, RapidEye, WorldView-2, WorldView-3, SPOT 5, among others) with different specifications and acquisition costs have been reported in published studies [42]. Studies using remote sensing techniques take advantage of available images to identify and detect invasive plants [43]. Remote sensing images record measurements of the energy reflected and absorbed by the surface of the Earth. For instance, multispectral images, such as those collected by satellite instruments as ESA's S2, contain detailed spectral and spatial information [44] that can be used to create maps of the distribution of invasive plants [45]. Some studies applied remote sensing methods to satellite imagery by taking advantage of available indices. For example, the normalized difference vegetation index (NDVI) [46] was used to detect water hyacinth in Lake Tana, Ethiopia, by using monthly S2 images. There, satellite MODIS data were used to evaluate NDVI trends, concluding that the expansion of invasive plants is favored by fluctuations at the lake level. In [47], the NDVI and the normalized difference water index were used to monitor the water hyacinth in Mondego river, Portugal, showing also the potential of multispectral S2 data to assist in the development of strategies for controlling the invasion of aquatic weeds. In [2], fractional vegetation cover was used to estimate the area invaded in Al Kabir river, Lebanon, using S2 time series.

The wide variety of existing machine learning algorithms allows for the detailed interpretation of remote sensing images [48]. Classification techniques exhibit the potential to automatically classify image pixels containing invasive species [49]. For example, in [50], a Naïve Bayes classifier was used to map water hyacinth in Saigon river, Vietnam. In [51], the random forest (RF) classifier was applied to S2 images allowing for the detection of water hyacinth (among other land covers). In [52], a linear discriminant analysis was used on S2 images acquired in the Greater Letaba river system, South Africa. An ensemble learning approach based on the RF algorithm was applied for the same purpose in [53]. DL algorithms, such as CNNs [54], offer flexibility in their architecture that are quite appealing for remote sensing data processing [55], but have not been widely applied to the detection of water hyacinth according to our knowledge.

In the context of the management of invasive plants in the Guadiana river, the competent institution has been monitoring the river by using aircraft flights, field data, and S2 images. In our previous work [41], we proposed a methodology for preprocessing, processing, and evaluation of satellite images using different machine learning/DL techniques to automatically detect aquatic invasive plants in the Guadiana river, Spain. Moreover, we carried out a comprehensive comparison between unsupervised and supervised classifiers, such as K-means, RF, and CNNs. In addition, we proposed a strategy to quantitatively assess classification performance in our context. This validation strategy consisted in generating a synthetic ground truth image from a high spatial resolution image, explained in detail in [56]. In this way, we demonstrated that aquatic invasive plants could be detected automatically. We also observed in the obtained classification maps and performance metrics that the CNN classifier achieved better detection accuracies than other classifiers. As a result, in this work, we adopt the CNN classifier as a baseline to perform multitemporal monitoring of water hyacinth in the Guadiana river.

III. Materials and Methods

Fig. 3 graphically shows the workflow adopted to monitor water hyacinth in the analyzed time series. After the acquisition of S2 images in the two-year period analyzed, a preprocessing of these images is carried out. Then, automatic detection of invasive plants takes place by means of a trained CNN (in fact, three different trained models are considered in this work according to different experiments). The final classification outputs are used for the monitoring stage, which provides the percentage of water hyacinth detected over time.

A. Study Area

A section of the Guadiana river affected by water hyacinth has been selected for experiments. The region of interest (ROI)

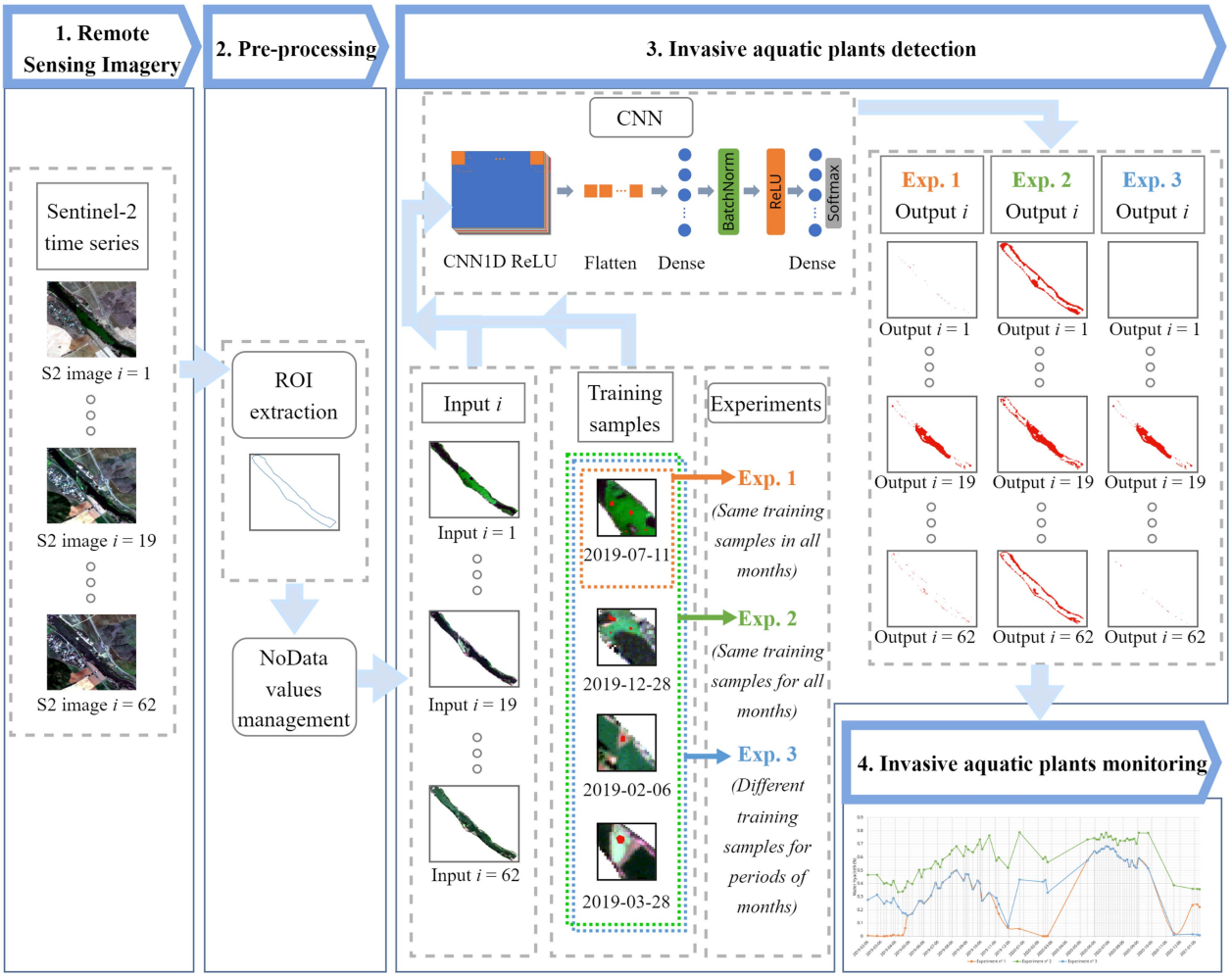

Fig. 3. Workflow of the procedure for monitoring the spatiotemporal distribution of water hyacinth in the Guadiana river using three different experiments. The architecture of the CNN used for mapping is also displayed.

TABLE I
DESCRIPTION OF S2 BANDS

Band name	B01	B02	B03	B04	B05	B06	B07	B08	B8A	B09	B10	B11	B12
Resolution (m)	60	10	10	10	20	20	20	10	20	60	60	20	20
Bandwidth (nm)	442.7	492.4	559.8	664.6	704.1	740.5	782.8	832.8	864.7	945.1	1373.5	1613.7	2202.4
Application	Coastal aerosol	Blue	Green	Red	Vegetation red edge	Vegetation red edge	Vegetation red edge	NIR	Narrow NIR	Water vapor	Cirrus	SWIR	SWIR

corresponds to an area affected by *Eichhornia crassipes*, close to the city of Mérida (ME_zone) in which an invasive plant control barrier has been installed in the river for mechanical removal. It covers an area of about 45 ha, between 38°50′ – 38° 51'N longitude and 6°19′ – 6° 18'W latitude (see Fig. 4), respectively.

B. Multitemporal Dataset

Among the advanced instruments capable of capturing the spectral response of the Earth's surface, satellites launched by ESA (as part as the Copernicus programme) have been incorporated in this study. The S2 mission provides open-access multispectral datasets that offer the potential to monitor water hyacinth in rivers [47]. In particular, the level-2 A (S2L2A) products (with atmospheric correction) of the time series described in Table III have been acquired from SentinelHub [57]. The S2L2A imagery is composed of 100×100 km^2 tiles in the Universal Transverse Mercator/World Geodetic System-84 projection, collected using a revisit time of five days. In Table I, we give the spatial and spectral resolutions of these images in each of the 12 available spectral bands. In our study, a period of two years has been monitored using a total of 62 S2 images (collected between January 2019 and January 2021), discarding those datasets in which the ROI was covered by clouds. Table II reports the final set of images used in our study.

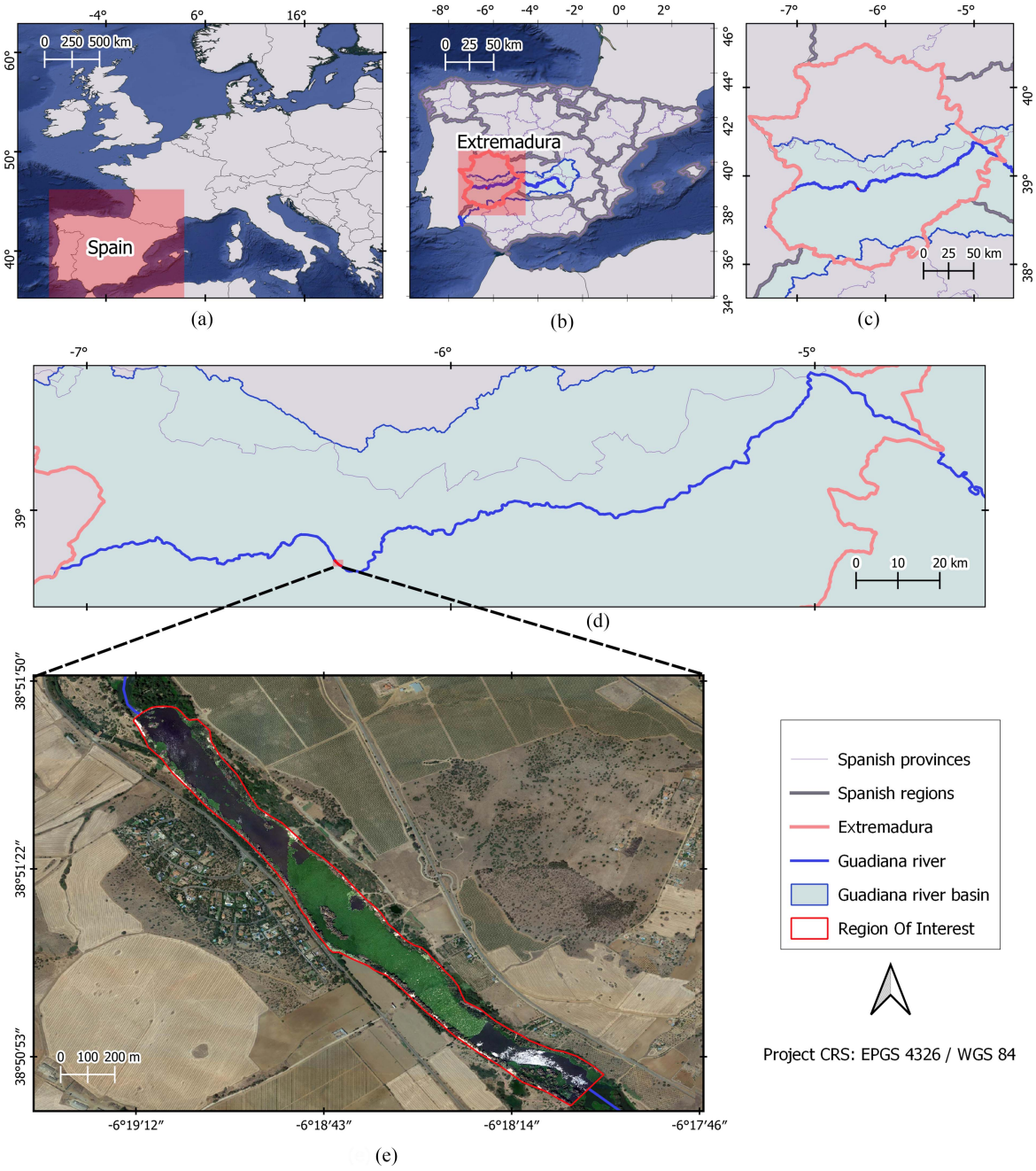

Fig. 4. (a) Geographical location of Spain. (b) Geographical location of the region of Extremadura, the Guadiana river, and the Guadiana river basin. (c) Zoom of Extremadura region, depicting the Guadiana river and its basin. (d) Zoom of the Guadiana river in the Extremadura region. (e) Zoom of a high-resolution image, including an area affected by water hyacinth, close to the city of Mérida.

TABLE II
S2 IMAGES PROCESSED PER MONTH AND YEAR

Year	Jan.	Feb.	Mar.	Apr.	May	Jun.	Jul.	Aug.	Sep.	Oct.	Nov.	Dec.	Total
2019	0	2	3	4	3	3	5	3	4	3	2	2	34
2020	0	3	0	0	1	6	6	5	3	0	1	0	25
2021	3	0	0	0	0	0	0	0	0	0	0	0	3
Total (images per month)	3	5	3	4	4	9	11	8	7	3	3	2	62

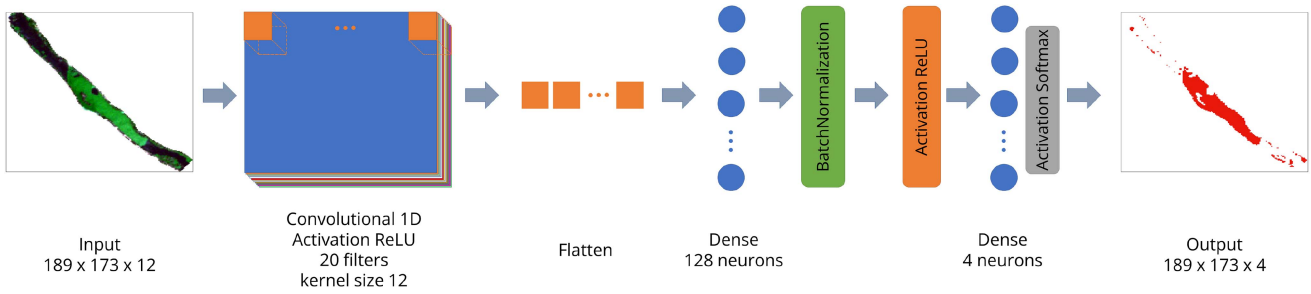

Fig. 5. Architecture of the considered CNN.

C. Hardware/Software Environment

The hardware environment in which our experiments were run comprises an Intel(R) Core(TM) i9-10900 k processor, 64-GB RAM memory, and 2-TB SSD. All the codes were implemented in Python 3.10 using TensorFlow and Keras frameworks. On the other hand, QGIS software was used for all preprocessing operations (such as raster clipping, image analysis, sample selection, etc.).

D. Image Preprocessing

After downloading the images, we manually extracted the ROIs in which we wanted to detect invasive plants. Resulting from the change of geometry to a dataset that does not have a square shape, pixels with no-data values appear. These no-data values are treated as explained in [41] to exclude them from training, prediction, and classification. For that purpose, a normalization of the pixel values of each band of the dataset has been carried out to scale them between 0 and 1. Furthermore, the format has been changed from 8 to 32 bits.

E. Image Analysis

We use a CNN algorithm to implement a model of water hyacinth detection, able to identify water hyacinth on S2 images and make predictions in other different images. CNNs have been widely used in spatial and spectral pattern analyses [55] to perform pixel classification studies, becoming a suitable algorithm for separating different vegetation types [58], [59], [60], [61]. Recent studies have demonstrated the effectiveness of CNNs in the task of mapping vegetation species in remote sensing images [62]. The CNN design consists of sets of blocks with neurons. The input data are transformed to an output volume of neurons connected through weights and biases. In this way, the output volume becomes the input of the next block [63]. The design of CNNs allows to process input data in the form of multiple arrays [64], including multispectral images. As the traditional multilayer perceptron, the CNN has hidden layers. There, patterns are exploited in at least one convolutional layer. Some studies apply CNNs to analyze the spatial patterns of the input image data. Others consider spectral information, and some works consider both the spatial and spectral information contained in the data [55]. In this study, the spectral pixels are considered as the input data. Our CNN architecture receives as many input vectors as pixels are present in the original S2 image. The adopted classification scheme is shown in Fig. 5 where our CNN architecture comprises the following layers.

1) A convolutional 1-D layer with ReLU activation, including 20 filters and kernel size of 12.
2) A reshaping (flatten) layer.
3) A fully connected (dense) layer with 128 neurons.
4) A batch normalization layer with ReLU activation.
5) A fully connected (dense) layer with four neurons and *Softmax* activation.

This architecture has achieved an overall classification accuracy of 90% when identifying aquatic invasive plants in our study area [41], outperforming other state-of-the-art methods.

As shown in Fig. 3, the CNN model has been trained with different training samples. The different training sets used by the CNN model define the three experiments performed in this work. The design of experiments 2 and 3 depends on the results of experiment 1. All conducted experiments are described in the following section.

IV. Experimental Results

A. Experimental Design

In order to detect water hyacinth in the Guadiana river, a multitemporal study has been carried out. A supervised CNN has been trained to process a two-year time series of S2 imagery. Before applying the CNN algorithm, we train the predictive model to be able to distinguish water hyacinth from other species and land covers. For this purpose, training samples of invasive plants have been collected, together with other training samples from different land cover types present in our case study. Three experiments are described as follows, where experiments 2 and 3 have been defined based on the results of water hyacinth detection in experiment 1.

1) Experiment 1: In this experiment, a single set of training samples are collected from an S2 image and used for prediction in the complete time series. First, to be able to identify the water hyacinth, the main land cover types present in the river have been identified by visual interpretation from a high-resolution image. For this purpose, we have chosen an orthophotograph acquired by the (Spanish) National Plan of Aerial Orthophotography (PNOA) using a photogrammetric flight. These flights are carried out over the whole Spanish territory. It has been obtained for free, from the National Geographic Institute [65]. The high spatial resolution PNOA dataset was collected in 2019. It is a multispectral image with three RGB bands of 7443 ×

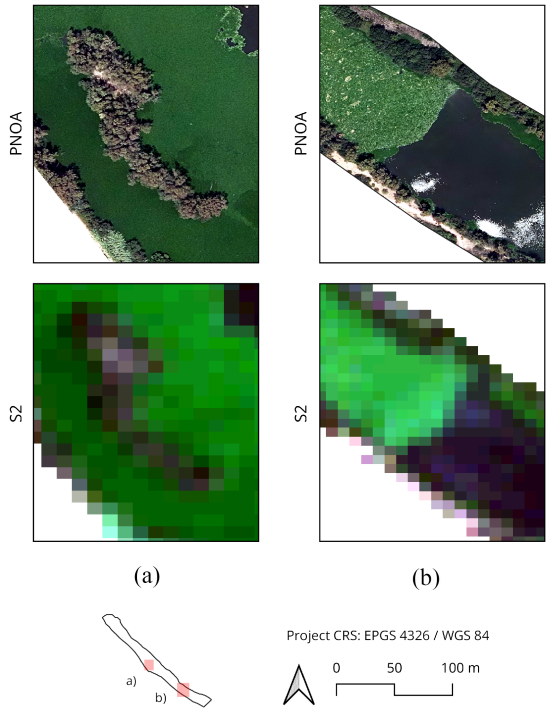

Fig. 6. (a) and (b) PNOA and S2 datasets. By visual interpretation, water hyacinth training samples are collected and differentiated from the rest of land cover types.

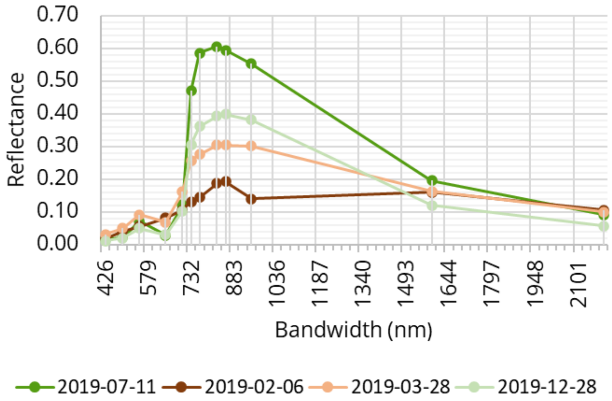

Fig. 7. Spectral signatures of the training samples of water hyacinth.

6321 pixels, in 8-bit format, with a spatial resolution of 0.25 m per pixel. Since the date of acquisition of the PNOA dataset belongs to the time series studied (July 2019), we have been able to accurately extract training samples on the July S2 image by using GIS tools. Specifically, we have collected training samples of water hyacinth and other land cover types from the ROI extracted from the image acquired by S2 on July 11, 2019. In this month, as shown in Fig. 2, water hyacinth is in a vegetative growth stage, and the plant can flower and produce fruits. As shown in Fig. 6, the high-resolution PNOA image acquired in July 2019 is suitable to separate the invasive plants from other species in the image. In this way, by visual interpretation, training samples can be collected by selecting those that belong to water hyacinth and those that belong to different land cover types (such as water, soil, and other kinds of vegetation).

The definition of the next experiments was established after analyzing the 62 images obtained after applying the CNN to each of the training sets. With the purpose of collecting a minimum number of samples from the S2 images, the results were considered acceptable when the detection of the invasive plants was adequate for all the months in the time series studied.

2) Experiment 2: In this experiment, we use a single set of training samples collected from several S2 images for predicting the presence of water hyacinth in the complete time series. Here, we consider a single training set (considering the different phenological stages of water hyacinth) for predicting its presence in every month in the multitemporal dataset. On the one hand, samples of different land cover types (except water hyacinth) were collected on July 11, 2019, from the S2 dataset by resorting to visual inspection of the high spatial resolution PNOA dataset and GIS techniques. We rely on field reports and technical consultations with CHG to conclude that the spatial resolution of S2 images is acceptable to collect water hyacinth samples by visual interpretation (from areas that are large enough and are fully occupied by the plant) on different phases of the vegetative cycle. In addition, to avoid collecting erroneous training samples, S2 images have been visualized with indices that highlight vegetation and water types (such as NDVI and moisture index). In this way, samples have been extracted at four different dates (since the training samples used in experiment 1 are not sufficient for a correct detection of the invasive plant in all the months of the year). These dates are as follows.

1) February 6, 2019, when the water hyacinth is in dormancy.
2) March 28, 2019, when it is in flowering stage.
3) July 11, 2019, when it is in vegetative growth.
4) December 28, 2019, when it is also in dormancy, but with different natural color.

The spectral signatures of water hyacinth in the dates reported above are shown in Fig. 7. They follow a similar trend as that of conventional spectral signatures of vegetation, with absorption features in the red and blue wavelengths and high reflectance in the green and near infrared (NIR) wavelengths [66]. Despite that, they exhibit notable differences that justify the collection of water hyacinth samples on different dates. As it is also shown on the RGB color composition of the S2 image in Fig. 10, the different water hyacinth colors depend on the vegetative cycle in which they are. There are significant variations in terms of reflectance in the RGB bands, especially in B03 (559.8 nm), justifying the color changes from green (vegetative growth stage) to brown (dormancy).

3) Experiment 3: In this experiment, we collected a set of training samples belonging to different phenological stages of the water hyacinth that notably affect its spectral signature. First, after analyzing all the images, we assumed that other land cover types are common in each training set, so they were extracted on July 11, 2019, by visual interpretation, as reported in previous experiments. Second, water hyacinth samples were acquired on the same dates, as in the previous experiment. On the contrary, every training set is considered just for a specific period of the

TABLE III
NUMBER OF TRAINING SAMPLES (PIXELS) USED IN OUR EXPERIMENTS

	Experiment 1	Experiment 2	Experiment 3			
			Period 1	Period 2	Period 3	Period 4
Water hyacinth	162	427	30	57	162	178
Other land cover types	288	288	288	288	288	288

year. Accordingly, the first training set (collected on February 6, 2019) is only considered for February. The second set (collected on March 28, 2019) is considered for March and April. The third one (collected on July 11, 2019) is used in the May–October period. Finally, the samples collected on December 28, 2019, are used in the November–January period.

Table III describes the different training sets considered in this experiment. Considering that an S2 image has 4471 labeled pixels and that there are a total of 62 images that have been processed, the number of training samples required for each experiment is quite small.

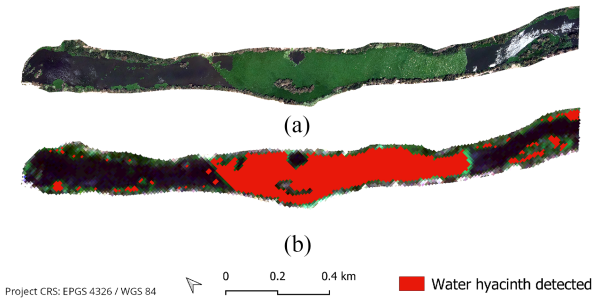

Fig. 8. (a) S2 image was collected at the same date as the PNOA reference image. (b) Water hyacinth detection results on the S2 image.

B. Experimental Results

This section describes the obtained detection results and justifies the consideration of different dates to collect training samples. Experiments 2 and 3 arise from the fact that new training samples need to be collected in order to reflect the phenological stage of the plant in different months of the year.

Fig. 9 shows the dynamics presented by the water hyacinth in the Guadiana river study areas. Specifically, it reports the detection results obtained after applying the CNN algorithm to four different cases, with four different training sets collected on different dates (i.e., July, December, February, and March). On the other hand, Fig. 10 displays some of the obtained invasive plant detection results with different training sets.

Regarding the results in Fig. 9, we note that the use of the training set collected on July 11, 2019, (referred to hereinafter as set 1, collected during the growing stage of the plant) reveals an increase in the percentage of pixels containing water hyacinth with regards to the ROI in May 2019. It can also be seen that the percentage of detected pixels reaches a maximum in the summer months. At this point, there is a slow decline (i.e., a decrease in the percentage of pixels labeled as water hyacinth in the ROI). Such decline is steeper in November, when the plant is in dormancy. In this case, the training samples were collected by visual interpretation using a high-resolution image (PNOA) from the same date. As a consequence, the detection results in Fig. 8 can be considered quite accurate. Particularly, the large mass of invasive plants accumulated behind the barrier is perfectly detected [see Fig. 10(a)]. On the contrary, when the training samples from February (set 2) and March (set 3) are used, the invasive plants are hardly detected. This can be seen in Fig. 9; with the July 2019 training set, almost no water hyacinth is detected in February and March. On the other hand, the use of training samples collected in December (set 4) also seems suitable for accurate detection of hyacinth in the S2 image acquired in July, as shown in Fig. 10(a). This is confirmed by the correlation of the plots obtained after using the December and July training sets in Fig. 9. However, no correlation can be appreciated from August to December.

According to the results in Fig. 9, with the set of samples collected in July, no hyacinth could be detected in February. However, as shown in Fig. 10, invasive plants can be seen in the S2 images. It should be noted that, in February, the hyacynth is in a period of vegetative standstill and has brown color. With the samples collected in February (set 2), the detection results are accurate. With the samples collected in March (set 3), the hyacinth can be also detected, but not in all covered areas. The same happens with the samples collected in December (set 4), i.e., the invasive plants cannot be detected in the February image.

As shown in Fig. 2, in March, the plant starts flowering. As shown in Fig. 9, with the samples collected in July, the plants are not detected in March. On the contrary, as shown in Fig. 10(c), the plant appears in brown and green colors. Consequently, there is a need to collect training samples in March, since set 3 is the only training set that allows for a correct detection of the water hyacinth in this period. In other words, to avoid nondetections of water hyacinth in February and March, we need training samples collected in those months (although the corresponding sets do not describe well the status of the plant in the rest of the months of the year).

Finally, as we can see in Fig. 10(d), the water hyacinth appears with green color in December and can only be correctly detected with the training samples collected on the same month (set 4). These detection results can also be appreciated in Fig. 9. Similar results were obtained in the two analyzed years, revealing that the seasonal behavior of water hyacinth is quite stable.

C. Interpretation of Water Hyacinth Dynamics

In this section, we discuss the dynamics of the invasive plant over time, taking as reference Fig. 11 that reports the detection

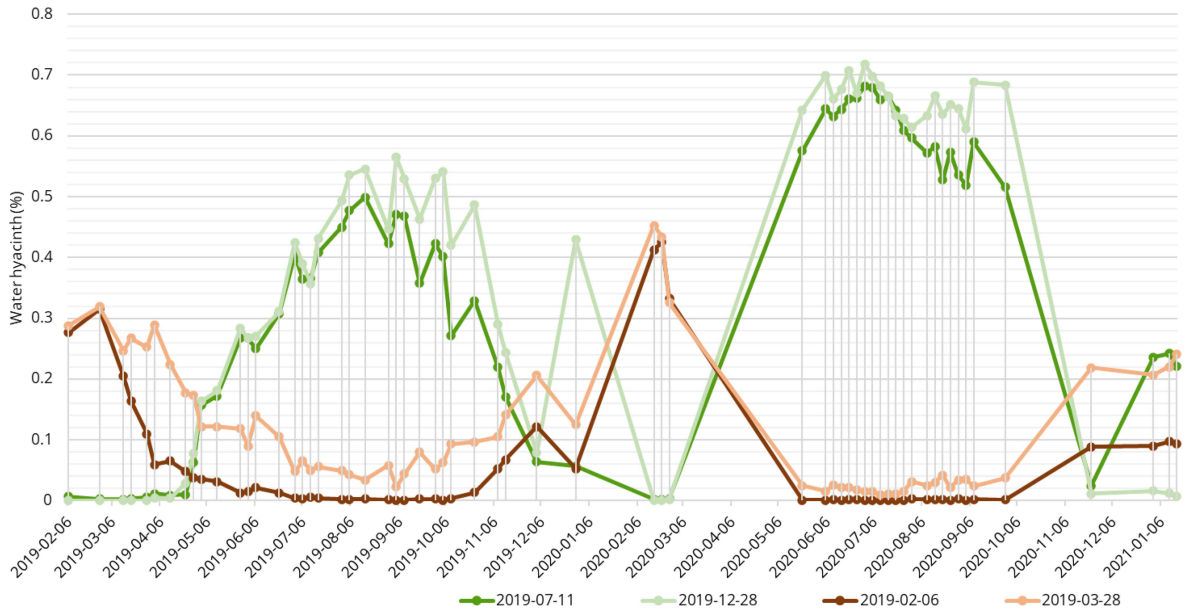

Fig. 9. Water hyacinth detection results (% of pixels detected in the ROI, excluding no-data values) for the time series (2019–2021) using the considered training sets: Set 1 (July 11, 2019), set 2 (February 6, 2019), set 3 (March 28, 2019), and set 4 (December 28, 2019).

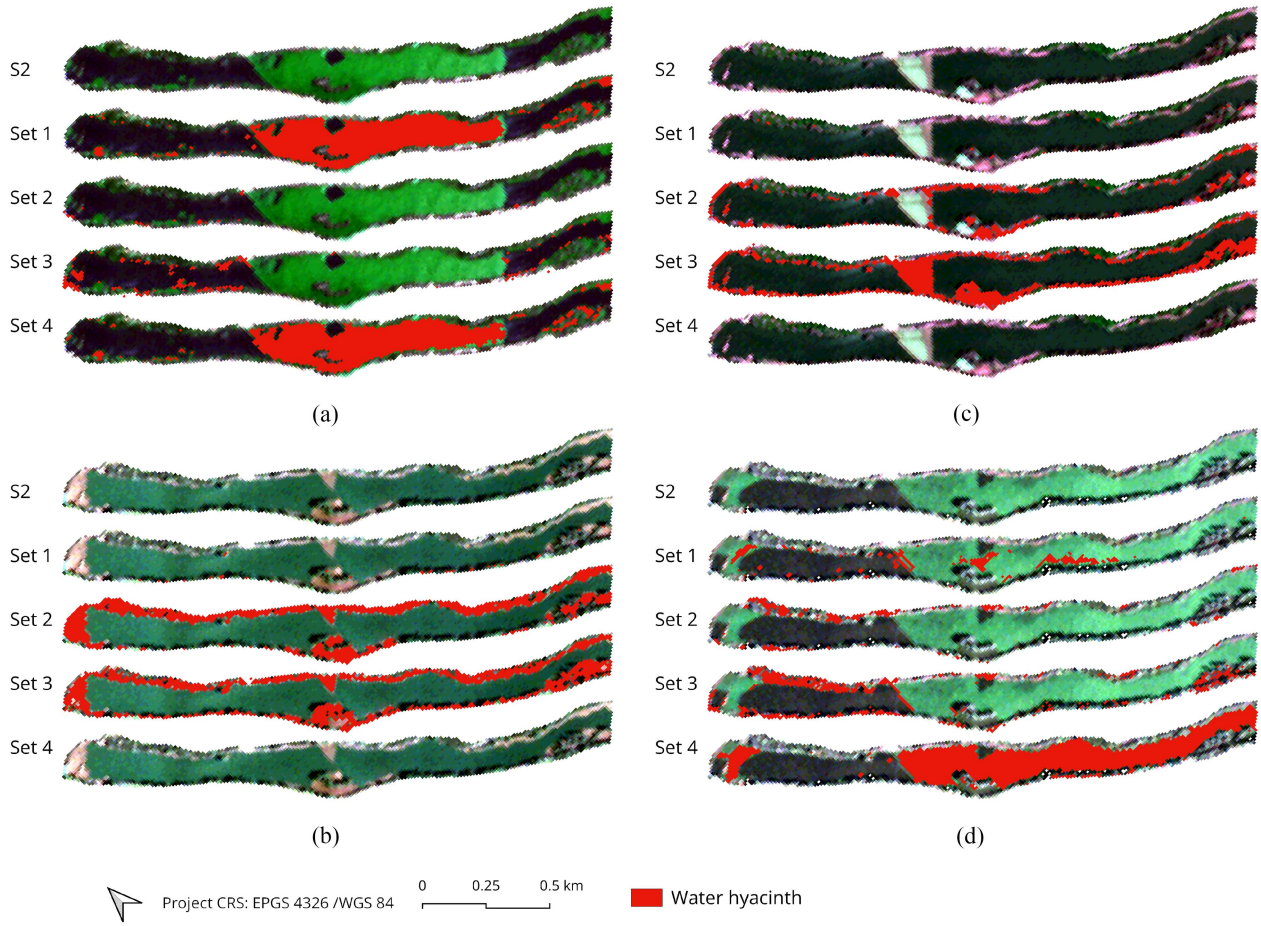

Fig. 10. Results obtained after applying the CNN to the S2 images acquired on the following dates. (a) July 11, 2019. (b) February 6, 2019. (c) March 28, 2019. (d) December 28, 2019. Pixels containing water hyacinth on the surface of the river are marked in red. For each image, we show the detection results obtained by using different training sets; samples collected on July 11, 2019 (set 1), February 6, 2019 (set 2), March 28, 2019 (set 3), and December 28, 2019 (set 4). The images are visualized in natural color (RGB).

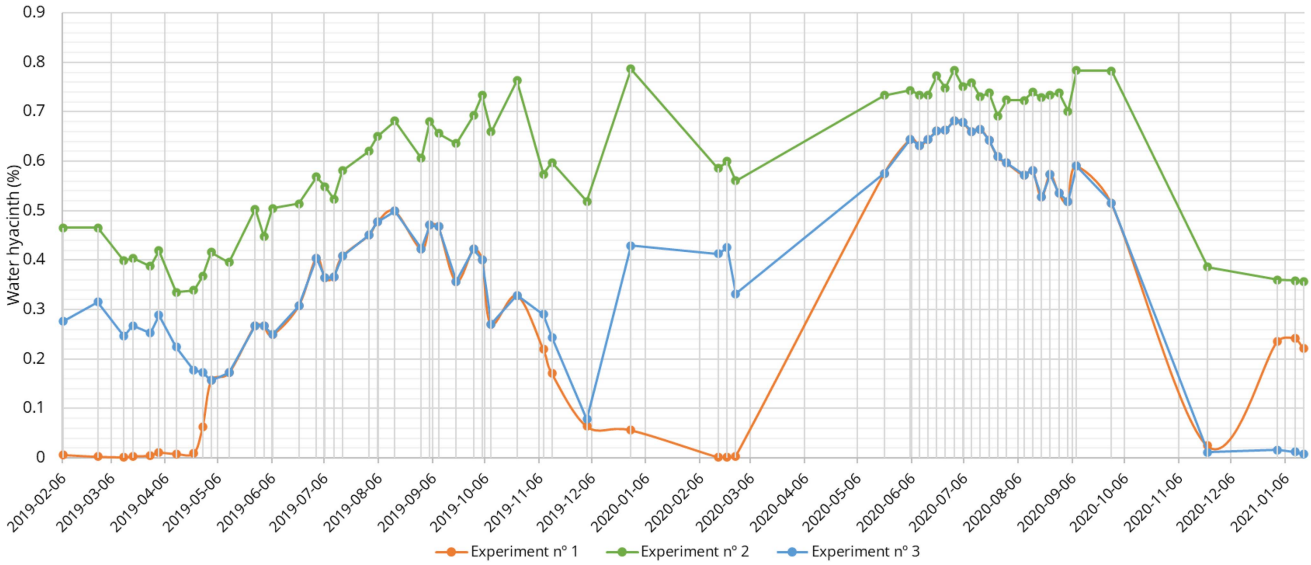

Fig. 11. Percentage of pixels of water hyacinth in the ROI (excluding no-data values) obtained for the full time series (2019–2021) in each considered experiment.

results over the complete time series for each considered experiment.

1) Experiment 1: The dynamics followed by the water hyacinth in the considered time series can be well-understood in the period from May to November. The plant first experiences a growth period, and then the percentage of pixels occupied by this invasive plant decreases. The increase is observed during the vegetative growth period of the plant, and the decrease happens when the vegetative rest period starts. On the contrary, little or no presence of water hyacinth was detected during the first months of the year (from January to May). Fewer invasive plants are also detected in December.

2) Experiment 2: This experiment also reveals an expected dynamic of increase and subsequent decrease of the number of pixels containing invasive plants in the input images collected along the year. Specifically, the percentage of pixels occupied by the invasive plant decreases until the vegetative growth period starts. When the change of vegetative growth phase happens, it increases until reaching a period of maximum occupancy, and then decreases again at the beginning of the vegetative dormancy phase.

3) Experiment 3: This experiment reveals a similar pattern as experiment 2. However, it is observed that the percentage of water hyacinth pixels decreases over the complete time series.

D. CNN Model Assessment

To assess that the considered CNN model can detect water hyacinth, this section conducts a more detailed assessment of such model. As shown in Fig. 8, the detection results obtained by the CNN can be assessed by comparisons with the PNOA high-resolution image. The S2 images allow identifying the masses of water hyacinth on the surface of the river (see Fig. 12). This visual verification has been complemented with reports provided from the CHG [30]. Moreover, the results are supported

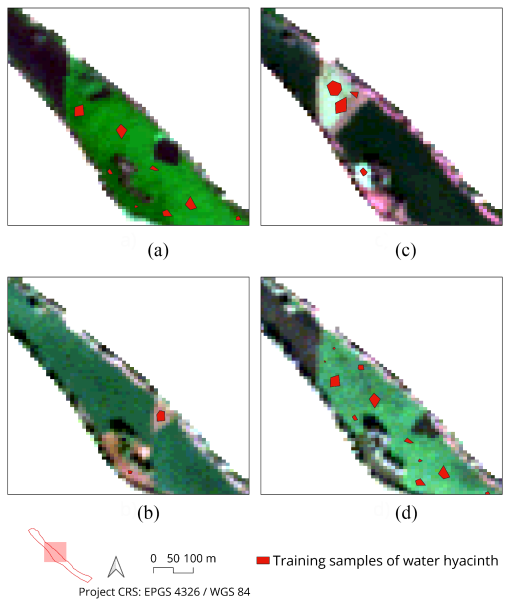

Fig. 12. Some training samples collected for water hyacinth in different training sets. (a) July 11, 2019 (set 1). (b) February 6, 2019 (set 2). (c) March 28, 2019 (set 3). (d) December 28, 2019 (set 4).

by the natural trend of the water hyacinth growth over the year, as shown in Fig. 2.

All the output images obtained by the CNN model in each experiment (a total of 186 images, 62 per experiment) have been carefully analyzed. However, we only display output images that exhibit important changes in the dynamics of the invasive plant for simplicity. These selected output images are shown in Fig. 13. Specifically, we show images from each experiment for different acquisition dates. Fig. 13 also includes a reproduction of Fig. 11 from the previous section to facilitate the evaluation of the results. Some considerations are given as follows for each individual experiment.

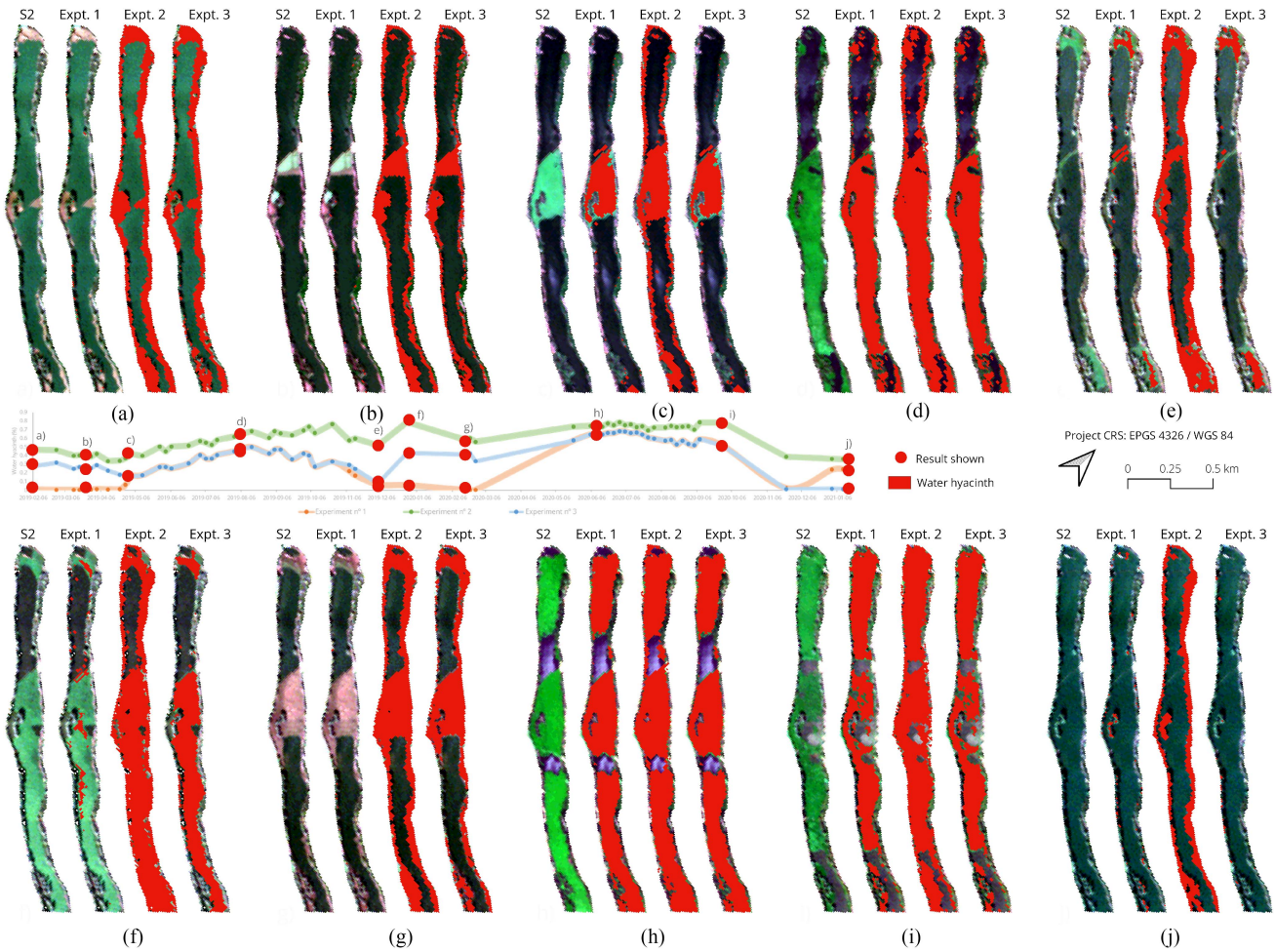

Fig. 13. Water hyacinth detection results on some acquisition dates included in the studied time series. (a) February 6, 2019. (b) March 28, 2019. (c) May 2, 2019. (d) August 5, 2019. (e) December 3, 2019. (f) December 28, 2019. (g) February 16, 2020. (h) June 10, 2020. (i) September 28, 2020. (j) January 16, 2020.

1) Experiment 1: It can be verified that with the set of training samples of experiment 1, no water hyacinth can be detected in the first months of the year (i.e., February and March) when it is present on the surface of the river. From May to October, the surface area detected by the CNN coincides with the one that can be seen in the satellite image. According to the CHG, the hyacinth reached its maximum occupation in the summer months [as shown in Fig. 13(d)]. In December, parts of the invasive plants that are present are actually detected [see Fig. 13(e) and (f)].

2) Experiments 2 and 3: In these two experiments, we detect all the water hyacinth that can be seen in the images acquired from S2 [as shown in Fig. 13(a)–(j)]. A sharp rise in the amount of hyacinth can be observed by the end of December, as it can be seen from the S2 image in Fig. 13(f). Far from being a prediction error, according to technical information from CHG technicians, on that date, the water hyacinth containment barrier was operating at full capacity, accumulating the invasive plants brought by the upstream current for its subsequent removal from the riverbed by mechanical means. Experiments 2 and 3 actually confirm this fact. In addition, according to the CHG reports, this study zone was considered to be free of invasive plants in December 2020, because they were removed with the change of phase. Taking into account this situation, CHG changed the status to *pre-eradication* and *early warning*. When we use the training samples collected in December (experiment 3), the obtained results indicate that the water surface is free from these plants on those dates.

V. Discussion

Results of experiment 1 reveal a successful monitoring of the study area affected by water hyacinth, because with only a few training samples (collected from a single S2 image), it was possible to detect the existing masses of invasive plants in the seasonal growth periods of the entire two-year period analyzed. The detection was not accurate on the periods of dormancy of these plants. However, if accurate detection of water hyacinth in all months of the year is necessary, experiments 2 and 3 are needed. As reported in [62], the temporal variations of the plant (due to its phenology) may limit the transferability of the predictive models through time. To avoid this, in this study, we collect training samples in specific months to consider multiple phenological phases of the plant. In other words, with a training set in which the water hyacinth samples come from the same date, it is not possible to detect water hyacinth in the

rest of the months of the year. As it was concluded in [43], the accuracy of aquatic weeds mapping by using remote sensing techniques can be improved by dividing the variability of species into phenological stages. Therefore, it is necessary to collect training samples in specific months in order to take into account the phenological behavior of the plant, which varies depending on the actual month being monitored.

In the analysis of S2 images from the time series considered in this study (2019–2021), checking the natural RGB color display (what the human eye perceives) can provide information about the state of the plant. During the months of January and February, when the plants are at the end of their phenological cycle, they appear in brown color. The plants become green in March and April. They remain green from May onwards, when they are in their vegetative growth stage, until the end of the year. It was therefore necessary to collect samples in July, December, February, and March to make sure that water hyacinth is properly detected throughout the year.

In order to choose the best training set for predicting the aquatic weeds in the time series, it was necessary to collect samples in December, February, and March. During these months, the aquatic weeds can be clearly seen, so it is easier to know where it is better to collect the training set from a specific date. This is particularly the case for February. In other dates, the detection results are not clear (e.g., with the March samples, we can obtain good detection results until the end of April).

Focusing on the color nature of the samples, our experiments reveal that samples with different colors are needed in order to obtain accurate detection results. This was suggested in [46]. It was also shown in [52] that the spectral signature of water hyacinth is clearly different in the wet and dry seasons. In our study, we found that samples from July allow for a correct identification of the plant when it appears in green color (from July to December). Quite opposite, when the plant appears in brown color, the detection results improve when we incorporate the training samples collected at the end of December, February, and March.

VI. Conclusion

In this work, we have modeled the spatiotemporal distribution of invasive plants (water hyacinth) in the Guadiana river (Spain) over the period 2019–2021. It has been shown that monitoring the distribution of hyacinth does not require field observations. In fact, the status of the plant can be monitored every five days using medium spatial resolution images, such as those collected by ESA's S2 satellite. We also demonstrated that it is only necessary to train the considered predictive model (CNN) once, using a high-resolution image (in our case, the PNOA image) to extract the most representative samples in the study area. This allows us to separate invasive plants from other land cover surfaces (such as water, soil, and other kinds of vegetation) for a period of at least two years. To detect the water hyacinth at different stages of its biological life cycle (considering that they exhibit different spectral signatures), a comprehensive training set was collected by visual interpretation of the S2 images. As a result, very few training samples are needed to make predictions in the subsequent year.

In future studies, we will consider other high spatial resolution images to quantitatively assess the obtained results via synthetic ground truth images.

Acknowledgment

The authors would like to thank CHG for providing monthly monitoring reports on the evolution of the water hyacinth, as well as information on the actions carried out in the study area, Tomás Rodríguez for providing photographs of the water hyacinth on the Guadiana river, and Associate Editor and the three Anonymous Reviewers for their outstanding comments and suggestions that greatly helped us to improve the technical presentation and content of our work.

References

[1] B. Gopal, *Water Hyacinth. (Aquatic Plant Studies 1)*. Cambridge, U.K.: Cambridge Univ. Press, 1987.

[2] Y. Ghoussein et al., "Multitemporal remote sensing based on an FVC reference period using Sentinel-2 for monitoring *Eichhornia crassipes* on a Mediterranean river," *Remote Sens.*, vol. 11, 2019, Art. no. 1856.

[3] A. Malik, "Environmental challenge *vis a vis* opportunity: The case of water hyacinth," *Environ. Int.*, vol. 33, pp. 122–138, 2007.

[4] N. Jafari, "Ecological and socio-economic utilization of water hyacinth (*Eichhornia crassipes Mart Solms*)," *J. Appl. Sci. Environ. Manage.*, vol. 14, 2010, Art. no. 57834.

[5] Q. Mahmood et al., "Lab scale studies on water hyacinth (*Eichhornia crassipes Marts Solms*) for biotreatment of textile wastewater," *Caspian J. Environ. Sci.*, vol. 3, pp. 83–88, 2005.

[6] A. M. Lissy and G. Madhu, "Removal of heavy metals from waste water using water hyacinth," *ACEEE Int. J. Transp. Urban Develop.*, vol. 1, 2011, Art. no. 48.

[7] J. Lu, Z. Fu, and Z. Yin, "Performance of a water hyacinth (*Eichhornia crassipes*) system in the treatment of wastewater from a duck farm and the effects of using water hyacinth as duck feed," *J. Environ. Sci.*, vol. 20, pp. 513–519, 2008.

[8] P. Saha, O. Shinde, and S. Sarkar, "Phytoremediation of industrial mines wastewater using water hyacinth," *Int. J. Phytoremediation*, vol. 19, pp. 87–96, Jan. 2017.

[9] W. H. Ting, I. A. Tan, S. F. Salleh, and N. A. Wahab, "Application of water hyacinth (*Eichhornia crassipes*) for phytoremediation of ammoniacal nitrogen: A review," *J. Water Process Eng.*, vol. 22, pp. 239–249, Apr. 2018.

[10] G. K. Gaurav, T. Mehmood, L. Cheng, J. J. Klemeš, and D. K. Shrivastava, "Water hyacinth as a biomass: A review," *J. Cleaner Prod.*, vol. 277, Dec. 2020, Art. no. 122214.

[11] F. Li et al., "Water hyacinth for energy and environmental applications: A review," *Bioresource Technol.*, vol. 327, May 2021, Art. no. 124809.

[12] A. Salas-Ruiz and M. del Mar Barbero-Barrera, "Performance assessment of water hyacinth–cement composite," *Construction Building Mater.*, vol. 211, pp. 395–407, Jun. 2019.

[13] N. Merry M. Mitan, *Water Hyacinth: Potential and Threat*, vol. 19. Amsterdam, The Netherlands: Elsevier, 2019, pp. 1408–1412.

[14] A. A. Adelodun, U. O. Hassan, and V. O. Nwachuckwu, "Environmental, mechanical, and biochemical benefits of water hyacinth (*Eichhornia crassipes*)," *Environ. Sci. Pollut. Res.* vol. 27, pp. 30210–30221, May 2020.

[15] Global Invasive Species Database. Accessed: Nov. 30, 2022. [Online]. Available: http://www.iucngisd.org/gisd/100_worst.php

[16] Y. O. Ouma, A. Shalaby, and R. Tateishi, "Dynamism and abundance of water hyacinth in the Winam Gulf of Lake Victoria: Evidence from remote sensing and seasonal-climate data," *Int. J. Environ. Stud.*, vol. 62, pp. 449–465, Aug. 2005.

[17] C. Perna and D. Burrows, "Improved dissolved oxygen status following removal of exotic weed mats in important fish habitat lagoons of the tropical Burdekin River floodplain, Australia," *Mar. Pollut. Bull.*, vol. 51, pp. 138–148, 2005.

[18] V. D. Tobias, J. L. Conrad, B. Mahardja, and S. Khanna, "Impacts of water hyacinth treatment on water quality in a tidal estuarine environment," *Biol. Invasions*, vol. 21, pp. 3479–3490, Dec. 2019.

[19] A. M. Villamagna and B. R. Murphy, "Ecological and socio-economic impacts of invasive water hyacinth (Eichhornia crassipes): A review," *Freshwater Biol.*, vol. 55, pp. 282–298, 2010.

[20] V. Mozaffarian and B. Yaghoubi, "New record of Eichhornia crassipes (water hyacinth) from north of Iran," *Rostaniha*, vol. 16, pp. 208–2011, 2015.

[21] J. Caudill, J. D. Madsen, W. Pratt, and C. Llp, "Operational aquatic weed management in the California Sacramento-San Joaquin River Delta," *J. Aquatic Plant Manage.*, vol. 59, pp. 112–122, 2021.

[22] E. V. Wyk and B. W. V. Wilgen, "The cost of water hyacinth control in South Africa: A case study of three options," *Afr. J. Aquatic Sci.*, vol. 27, pp. 141–149, Jan. 2002.

[23] B. Greenfield, M. Blankinship, and T. McNabb, "Control costs, operation, and permitting issues for non-chemical plant control: Case studies in the San Francisco bay-delta region, California," *J. Aquatic Plant Manage.*, vol. 44, pp. 40–49, 2006.

[24] B. K. Greenfield, G. S. Siemering, J. C. Andrews, M. Rajan, S. P. Andrews, and D. F. Spencer, "Mechanical shredding of water hyacinth (Eichhornia crassipes): Effects on water quality in the Sacramento-San Joaquin River Delta, California," *Estuaries Coasts*, vol. 30, pp. 627–640, 2007.

[25] M. P. Hill and J. A. Coetzee, "Integrated control of water hyacinth in Africa 1," *EPPO Bull.*, vol. 38, pp. 452–457, 2008.

[26] J. jun Chu, Y. Ding, and Q. jia Zhuang, "Invasion and control of water hyacinth (*Eichhornia crassipes*) in China," *J. Zhejiang Univ. Sci. B*, vol. 7, pp. 623–626, 2006.

[27] N. J. Waltham and S. Fixler, "Aerial herbicide spray to control invasive water hyacinth (*Eichhornia crassipes*): Water quality concerns fronting fish occupying a tropical floodplain wetland," *Trop. Conservation Sci.*, vol. 10, Dec. 2017. [Online]. Available: https://journals.sagepub.com/doi/epub/10.1177/1940082917741592

[28] M. H. Julien, "Biological control of water hyacinth with arthropods: A review to 2000," in *Proc. ACIAR*, 2000, pp. 8–20.

[29] J. A. Coetzee and M. P. Hill, "The role of eutrophication in the biological control of water hyacinth, *Eichhornia crassipes*, in South Africa," *BioControl*, vol. 57, no. 2, pp. 247–261, Apr. 2012.

[30] Confederación Hidrográfica del Guadiana O. A. Ministerio para la transición ecológica y el reto demográfico. Gobierno de España. Accessed: Nov. 30, 2022. [Online]. Available: https://www.chguadiana.es/cuenca-hidrografica/especies-exoticas-invasoras/actuaciones

[31] L. A. Wainger et al., "Evidence-based economic analysis demonstrates that ecosystem service benefits of water hyacinth management greatly exceed research and control costs," *PeerJ*, vol. 6, 2018, Art. no. e4824.

[32] Z. H. Zhang and J. Y. Guo, "Biology of water hyacinth," *Water Hyacinth*, 1st Ed., 2017, pp. 1–29.

[33] Centre for Agricultural Bioscience International– *Eichhornia Crassipes* (Water Hyacinth). Accessed: Nov. 30, 2022. [Online]. Available: https://www.cabi.org/isc/datasheet/20544#tosummaryOfInvasiveness

[34] T. R. Téllez, E. M. de Rodrigo López, G. L. Granado, E. A. Pérez, R. M. López, and J. M. S. Guzmán, "The water hyacinth, *Eichhornia crassipes*: An invasive plant in the Guadiana river basin (Spain)," *Aquatic Invasions*, vol. 3, pp. 42–53, 2008.

[35] E. P. Albano and D. T. R. Téllez, "Reproducción sexual del jacinto de agua (*Eichhornia crassipes*): Germinación, anatomía y banco de semillas," Ph.D. dissertation, Departamento de Biología Vegetal, Ecología y Ciencias de la Tierra. Grupo de Investigación en Biología de la Conservación, Universidad de Extremadura, Badajoz, Spain, 2012.

[36] E. A. Pérez et al., "Seed germination and risks of using the invasive plant *Eichhornia crassipes* (Mart.) Solms-Laub. (water hyacinth) for composting, ovine feeding and biogas production," *Acta Botanica Gallica*, vol. 162, pp. 203–214, Jul. 2015.

[37] J. D. Madsen, G. M. Morgan, and john Miskella, "Seasonal growth and phenology of water hyacinth, curlyleaf pondweed, and Brazilian egeria in the Sacramento-San Joaquin River Delta," *Article J. Aquatic Plant Manage.*, vol. 59, pp. 16–27, 2021.

[38] T. D. Center and N. R. Spencer, "The phenology and growth of water hyacinth (*Eichhornia crassipes* (Mart.) Solms) in a eutrophic north-central Florida lake," *Aquatic Botany*, vol. 10, pp. 1–32, 1981.

[39] E. A. Pérez, J. A. Coetzee, T. R. Téllez, and M. P. Hill, "A first report of water hyacinth (*Eichhornia crassipes*) soil seed banks in South Africa," *South Afr. J. Botany*, vol. 77, pp. 795–800, Aug. 2011.

[40] D. Eva, A. Pérez, and D. T. R. Téllez, "Reproducción sexual del jacinto de agua (*Eichhornia crassipes*): Germinación, anatomía y banco de semillas," Ph.D. dissertation, Departamento de Biología Vegetal, Ecología y Ciencias de la Tierra. Grupo de Investigación en Biología de la Conservación, Universidad de Extremadura, Badajoz, Spain, 2012.

[41] E. C. Rodríguez-Garlito, A. Paz-Gallardo, and A. Plaza, "Automatic detection of aquatic weeds: A case study in the Guadiana River, Spain," *IEEE J. Sel. Topics Appl. Earth Observ. Remote Sens.*, vol. 15, pp. 8567–8585, Sep. 2022.

[42] K. H. Thamaga and T. Dube, "Remote sensing of invasive water hyacinth (*Eichhornia crassipes*): A review on applications and challenges," *Remote Sens. Appl.: Soc. Environ.*, vol. 10, pp. 36–46, 2018.

[43] E. L. Hestir et al., "Identification of invasive vegetation using hyperspectral remote sensing in the california delta ecosystem," *Remote Sens. Environ.*, vol. 112, pp. 4034–4047, 2008.

[44] A. Plaza, J. Plaza, A. Paz, and S. Sánchez, "Parallel hyperspectral image and signal processing [applications corner]," *IEEE Signal Process. Mag.*, vol. 28, no. 3, pp. 119–126, May 2011.

[45] C. Joshi, J. D. Leeuw, and I. C. V. Duren, "Remote sensing and GIS applications for mapping and spatial modelling of invasive species," in *Proc. Int. Soc. Photogrammetry Remote Sens.*, 2004, pp. 669–677.

[46] M. G. Dersseh et al., "Spatial and temporal dynamics of water hyacinth and its linkage with lake-level fluctuation: Lake Tana, a sub-humid region of the Ethiopian Highlands," *Water*, vol. 12, Jul. 2020, Art. no. 1435.

[47] R. Gerardo and I. P. D. Lima, "Assessing the potential of Sentinel-2 data for tracking invasive water hyacinth in a river branch," *J. Appl. Remote Sens.*, vol. 16, 2022, Art. no. 014511.

[48] P. Ghamisi, J. Plaza, Y. Chen, J. Li, and A. J. Plaza, "Advanced spectral classifiers for hyperspectral images: A review," *IEEE Geosci. Remote Sens. Mag.*, vol. 5, no. 1, pp. 8–32, Mar. 2017.

[49] A. Datta et al., "Monitoring the spread of water hyacinth (*pontederia crassipes*): Challenges and future developments," *Front. Ecol. Evol.*, vol. 9, Jan. 2021, Art. no. 631338.

[50] N. Janssens, L. Schreyers, L. Biermann, M. V. D. Ploeg, T. K. L. Bui, and T. V. Emmerik, "Rivers running green: Water hyacinth invasion monitored from space," *Environ. Res. Lett.*, vol. 17, 2022, Art. no. 044069.

[51] C. Ade, S. Khanna, M. Lay, S. L. Ustin, and E. L. Hestir, "Genus-level mapping of invasive floating aquatic vegetation using Sentinel-2 satellite remote sensing," *Remote Sens.*, vol. 14, Jun. 2022, Art. no. 3013.

[52] K. H. Thamaga and T. Dube, "Understanding seasonal dynamics of invasive water hyacinth (*Eichhornia crassipes*) in the greater Letaba river system using Sentinel-2 satellite data," *GIScience Remote Sens.*, vol. 56, pp. 1355–1377, Nov. 2019.

[53] G. Singh, C. Reynolds, M. Byrne, and B. Rosman, "A remote sensing method to monitor water, aquatic vegetation, and invasive water hyacinth at national extents," *Remote Sens.*, vol. 12, Dec. 2020, Art. no. 4021.

[54] I. Goodfellow, Y. Bengio, and A. Courville, *Deep Learning*. Cambridge, MA, USA: MIT Press, 2016.

[55] M. E. Paoletti, J. M. Haut, J. Plaza, and A. Plaza, "Deep learning classifiers for hyperspectral imaging: A review," *ISPRS J. Photogrammetry Remote Sens.*, vol. 158, pp. 279–317, 2019.

[56] E. C. Rodríguez-Garlito and A. Paz-Gallardo, "Efficiently mapping large areas of olive trees using drones in Extremadura, Spain," *IEEE J. Miniaturization Air Space Syst.*, vol. 2, no. 3, pp. 148–156, Sep. 2021.

[57] SentinelHub. Accessed: Nov. 30, 2022. [Online]. Available: https://www.sentinel-hub.com

[58] S. M. Sharpe, A. W. Schumann, J. Yu, and N. S. Boyd, "Vegetation detection and discrimination within vegetable plasticulture row-middles using a convolutional neural network," *Precis. Agriculture*, vol. 21, pp. 264–277, Apr. 2020.

[59] N. Flood, F. Watson, and L. Collett, "Using a U-Net convolutional neural network to map woody vegetation extent from high resolution satellite imagery across queensland, Australia," *Int. J. Appl. Earth Observ. Geoinformation*, vol. 82, Oct. 2019, Art. no. 101897.

[60] U. Bayr and O. Puschmann, "Automatic detection of woody vegetation in repeat landscape photographs using a convolutional neural network," *Ecological Inform.*, vol. 50, pp. 220–233, Mar. 2019.

[61] Y. Jiang, S. M. Asce, Y. Bai, F. Asce, and S. Han, "Determining ground elevations covered by vegetation on construction sites using drone-based orthoimage and convolutional neural network," *J. Comput. Civil Eng.*, vol. 34, no. 6, 2020.

[62] T. Kattenborn, J. Leitloff, F. Schiefer, and S. Hinz, "Review on convolutional neural networks (CNN) in vegetation remote sensing," *ISPRS J. Photogrammetry Remote Sens.*, vol. 173, pp. 24–49, Mar. 2021.

[63] M. E. Paoletti, J. M. Haut, J. Plaza, and A. Plaza, "A new deep convolutional neural network for fast hyperspectral image classification," *ISPRS J. Photogrammetry Remote Sens.*, vol. 145, pp. 120–147, 2018.

[64] Y. Lecun, Y. Bengio, and G. Hinton, "Deep learning," *Nature*, vol. 521, pp. 436–444, 2015.
[65] Plan nacional de ortofotografía aérea. Accessed: Nov. 30, 2022. [Online]. Available: https://pnoa.ign.es
[66] M. Govender, K. Chetty, and H. Bulcock, "A review of hyperspectral remote sensing and its application in vegetation and water resource studies," *Water SA*, vol. 33, pp. 145–151, 2007.

Elena C. Rodríguez-Garlito (Student Member, IEEE) received the B.Sc. degree in civil engineering and the M.Sc. degree in geographical information systems and RS, in 2013 and 2014, respectively, from the University of Extremadura, Cáceres, Spain, where she is currently working toward the Ph.D. degree with predoctoral contracts for the training of doctors in public RD centers belonging to the Extremadura System of Science, Technology, and Innovation and working on the development of machine/deep learning algorithms for invasive aquatic plants detection and natural resources management, using remote sensing data from satellites and drones.

She is currently a Member of Hyperspectral Computing Laboratory, Department of Technology of Computers and Communications, University of Extremadura. Her research interests include GIS, remote sensing, and machine/deep learning.

Abel Paz-Gallardo received the B.S. degree in computer engineering and the M.Sc. and Ph.D. degrees in computer science from the University of Extremadura, Cáceres, Spain, in 2007, 2009, and 2011, respectively.

During 2006 and 2007, he was a Research Assistant with Computer Architecture Department, University of Extremadura, where he became an Associate Professor in 2008. At the same time, he started working with Minimally Invasive Surgery Center Jesús Usón, Cáceres. In 2010, he started working with Bull Spain S.A., to deploy at CETA-Ciemat, Trujillo, Spain, the biggest GPGPU Cluster in Spain and one of the biggest ones in Europe. Since November 2010, he has been an Associate Professor with Computer Architecture Department. From October 2011 to July 2018, he was an IT Manager (CIO) of CETA-Ciemat, where he achieved the GPU Research Centre mention from NVIDIA as Principal Investigator. Since July 2018, he has been a Chief Information Officer of Greenfield Technologies, a precision agriculture company that provides recommendations to farmers, through the use of different innovative technologies (such as drones, satellites, sensors, and artificial intelligence) and applied research. He has participated in more than 40 international projects and has authored or coauthored more than 40 publications, including 16 journal citation report (JCR) papers (most of them published by IEEE journals) and more than 30 peer-reviewed international conference papers. His research interests include remotely sensed hyperspectral image analysis, signal processing, and efficient implementations of large-scale scientific problems on high-performance computing architectures, such as clusters and graphical processing units.

Prof. Paz-Gallardo was the recipient of the IEEE Signal Processing Magazine Best Column Award Paper from the IEEE Signal Processing Society in November 2015.

Antonio Plaza (Fellow, IEEE) received the M.Sc. and Ph.D. degrees in computer engineering from the University of Extremadura, Cáceres, Spain, in 1999 and 2002, respectively.

He is currently a Full Professor and the Head of Hyperspectral Computing Laboratory, Department of Technology of Computers and Communications, University of Extremadura. He has authored or coauthored more than 700 publications in the field of his research interests, including 381 JCR journal papers, 24 book chapters, and 330 peer-reviewed conference proceeding papers, and also guest edited ten special issues on hyperspectral remote sensing for different journals. His research interests include hyperspectral data processing and parallel computing of remote sensing data.

Prof. Plaza was the recipient of the recognition of Best Reviewers of *IEEE Geoscience and Remote Sensing Letters* (in 2009), the recognition of Best Reviewers of the IEEE TRANSACTIONS ON GEOSCIENCE AND REMOTE SENSING (in 2010) for which he was an Associate Editor (in 2007–2012), the Best Column Award of the IEEE Signal Processing Magazine in 2015, the 2013 Best Paper Award of the JSTARS journal, the most highly cited paper (2005–2010) in the *Journal of Parallel and Distributed Computing*, and best paper awards at the IEEE Workshop on Hyperspectral Image and Signal Processing: Evolution in Remote Sensing, the IEEE International Conference on Space Technology, and the IEEE Symposium on Signal Processing and Information Technology. He is also an Associate Editor for IEEE ACCESS (receiving the recognition of Outstanding Associate Editor for the journal in 2017) and was also Member of the Editorial Board of the *IEEE Geoscience and Remote Sensing Newsletter* (2011–2012) and *IEEE Geoscience and Remote Sensing Magazine* (2013). He was a Member of the steering committee of the IEEE JOURNAL OF SELECTED TOPICS IN APPLIED EARTH OBSERVATIONS AND REMOTE SENSING (JSTARS). He was the Director of Education Activities for the IEEE Geoscience and Remote Sensing Society (GRSS) (in 2011–2012), and the President of the Spanish Chapter of IEEE GRSS (in 2012–2016). He is a Chair of the Publications Awards Committee of IEEE GRSS and a Vice-Chair of the Fellow Evaluations Committee of IEEE GRSS. He has reviewed more than 500 manuscripts for more than 50 different journals. He was the Editor-in-Chief for IEEE TRANSACTIONS ON GEOSCIENCE AND REMOTE SENSING for five years (2013–2017) and IEEE JOURNAL ON MINIATURIZATION FOR AIR AND SPACE SYSTEMS (2019–2020). He has been included in the 2018–2021 Highly Cited Researchers List (Clarivate Analytics). He is a Fellow of IEEE "for contributions to hyperspectral data processing and parallel computing of Earth observation data" and a Member of Academia Europaea, The Academy of Europe.